JOURNAL OF AIRCRAFT
Vol. 41, No. 6, November–December 2004

State-Space Model Generation for Flexible Aircraft

Timothy A. Smith,* James W. Hakanson,† and Satish S. Nair‡
University of Missouri, Columbia, Missouri 65211
and
Rudolph N. Yurkovich§
The Boeing Company, St. Louis, Missouri 63166

Accurate simplification of the equations of motion of an aircraft, in a way that incorporates aeroelastic effects, is important to facilitate the development of reliable time-domain dynamic models. Such time-domain models are useful for control design and for the prediction of dynamic loads early in the design cycle. Various techniques reported in the literature for such model development are critically reviewed. A particular example case is used to illustrate the different methods. The issues involved are highlighted, and two possible error quantification methods are suggested.

Nomenclature

$\boldsymbol{A}_{i,j}, \boldsymbol{B}_i$	=	submatrices of the state A and B matrices
$a_{i,j}, b_{i,j}, c_{i,j}, d_{i,j}$	=	i, jth elements of the state space model $\boldsymbol{A}$, $\boldsymbol{B}$, $\boldsymbol{C}$, and $\boldsymbol{D}$ matrices
b	=	$\bar{c}/2$
$\bar{c}$	=	reference chord length
$\boldsymbol{H}(s)$	=	system transfer function matrix
$\hat{h}_{i,j}(s)$	=	i, jth element of the system transfer function matrix
J_1	=	cost function for the rational function approximation (RFA) error
J_2	=	cost function for the frequency response approximation error
j	=	square root of -1
k	=	nondimensional frequency, $\omega b/V$
k_{fi}, k_{ri}	=	RFA parameters
M	=	Mach number
$\boldsymbol{M}, \boldsymbol{C}, \boldsymbol{K}$	=	generalized structural matrices ($n \times n$)
n	=	system order
n_I	=	number of system inputs
n_O	=	number of system outputs
$\boldsymbol{P}_j$	=	rational function approximation matrix
$\boldsymbol{Q}(s)$	=	generalized aerodynamic forcing matrix ($n \times n$)
$\boldsymbol{Q}^I(s)$	=	imaginary part of the generalized aerodynamic forcing matrix
$\boldsymbol{Q}^R(s)$	=	real part of the generalized aerodynamic forcing matrix
$\boldsymbol{Q}_\delta(s)$	=	generalized control surface aerodynamic forcing matrix ($n \times m$)
$\bar{q}$	=	dynamic pressure, $\frac{1}{2}\rho V^2$
$\boldsymbol{R}$	=	lag state matrix
$\boldsymbol{r}$	=	vector of rigid-body displacements
s	=	Laplace variable
s'	=	nondimensional Laplace variable, sb/V
V	=	aircraft velocity
$\boldsymbol{x}$	=	generalized coordinate vector
$\boldsymbol{x}_a$	=	aerodynamic lag state vector
$\boldsymbol{y}(s)$	=	system output vector
γ	=	RFA lag parameter
$\boldsymbol{\delta}, \dot{\boldsymbol{\delta}}, \ddot{\boldsymbol{\delta}}$	=	control surface deflection, rate, and acceleration vectors, respectively
$\varepsilon_{1,ijk}, \varepsilon_{2,ijk}$	=	elements of the RFA and transfer matrix error matrices, respectively
$\boldsymbol{\zeta}$	=	vector of flexible mode displacements
$\boldsymbol{\eta}$	=	vector of flexible mode rates
ρ	=	air density

Received 8 October 2000; accepted for publication 18 December 2003.

*Engineer, Phantom Works.
†Ph.D. Student, Department of Mechanical and Aerospace Engineering.
‡Professor, Department of Mechanical and Aerospace Engineering.
§Boeing Senior Technical Fellow, Structures Technology Department, Fellow AIAA.

I. Introduction

THE time-domain representation of the generalized forces equations (GFE) of motion for an aircraft consists of a system of second-order matrix differential equations in a mixed time–frequency domain formulation:

$$\boldsymbol{M}\ddot{\boldsymbol{x}} + \boldsymbol{C}\dot{\boldsymbol{x}} + \boldsymbol{K}\boldsymbol{x} = \bar{q}\boldsymbol{Q}(M,k)\boldsymbol{x} - \boldsymbol{M}_\delta\ddot{\boldsymbol{\delta}} + \bar{q}\boldsymbol{Q}_\delta(M,k)\boldsymbol{\delta} \quad (1)$$

All terms in Eq. (1) are in the time domain, except the generalized aerodynamic forcing (GAF) matrices $\boldsymbol{Q}$ and $\boldsymbol{Q}_\delta$, which are functions of reduced frequency k and Mach number M. The GFE in the Laplace domain is

$$[\boldsymbol{M}s^2 + \boldsymbol{C}s + \boldsymbol{K}]\boldsymbol{x}(s) = \bar{q}\boldsymbol{Q}(s')\boldsymbol{x}(s) - \left[\boldsymbol{M}_\delta s^2 + \bar{q}\boldsymbol{Q}_\delta(s')\right]\boldsymbol{\delta}(s) \quad (2)$$

The GAF matrices are determined by oscillatory linear aerodynamic methods such as the doublet lattice method. They are determined at discrete values of the reduced frequency and are interpolated at any desired value of the reduced frequency. Because the GAF data are tabular in form, a time-domain representation of the system is not attainable through an inverse Laplace transform.

The traditional approach to obtain a time-domain model for the system entails the frequency domain approximation of the GAF data over the reduced frequency range of interest.[1–8] These approximations, generally known as rational function approximations (RFA), are continuous frequency domain functions optimized, in a least-squares sense, to approximate the GAF data.

Several RFA methods have been developed, of which three will be discussed herein. They are Roger's method,[2] the matrix Padé approximation (see Refs. 3 and 4), and Karpel's minimum-state method.[5–8] The main drawback to the use of RFA for approximation of the GAF matrices in the frequency domain is that modeling them accurately necessitates the introduction of additional aerodynamic states to the system. These additional states are known as lag states, and they are attributable to the effects that the aircraft wake induces on the structure. The addition of such lag states increases model size and computation time. For simplicity, the effect of aerodynamic forcing on the structure due to control surface motion is omitted in the following discussion because the RFA techniques can be easily extended to the case of control surface aerodynamic forcing.

Efforts to obtain an accurate time-domain model for aircraft loads and trajectory without the need for lag states has been the subject of much research. Two methods that have been developed for the generation of linear, time-invariant, state-space models for aircraft that do not need the introduction of lag states are flexible aircraft modeling using state space (FAMUSS)[9,10] and the P-transform method.[11,12] FAMUSS uses the result of a p-k flutter solution to construct the $\boldsymbol{A}$ matrix and employs linear and nonlinear curve fitting techniques to obtain the best match to a matrix transfer function frequency response direct solution through iteration on the $\boldsymbol{B}$, $\boldsymbol{C}$, and $\boldsymbol{D}$ matrices of a state model of a given size. The direct solution is obtained when the GAF data are splined and the system response is evaluated over the reduced frequency range of interest. The P-transform method uses the results of a p-k flutter solution to construct the state $\boldsymbol{A}$ and $\boldsymbol{B}$ matrices through a compilation of the modal response at each mode's resonant frequency.

RFA techniques, FAMUSS, and P-transform are by no means an exhaustive set of tools for the approximation of unsteady aerodynamics. Other methods such as Volterra series,[13] proper orthogonal decomposition,[14] indicial response,[15,16] and neural network approximation[17] have received much attention in the literature. One elegant solution to the approximation of the unsteady aerodynamics is presented by Leishman[15] and Leishman and Crouse.[16] The coefficients of the indicial (step) response of the relevant aerodynamic equations are fit to best match the aerodynamic forcing data. This method also leads to an linear time-invariant (LTI) model of the aircraft dynamics. The main difference between the indicial response method and the techniques discussed hereafter is that, in general, the aerodynamic forcing matrices are obtained in a generalized or modal coordinate system. To apply the indicial response method, the aerodynamics are transformed to the physical aircraft coordinates. The methods discussed herein perform the aerodynamic approximations in the generalized coordinate system.

This paper focuses on a technical review of the RFA, FAMUSS, and P-transform techniques. These were chosen for their traditional value (RFA) and for their value as design and analysis tools to the aerodynamic/aeroelastic modeling and controls communities (FAMUSS and P-transform). Subsequently, comparisons of the RFA methods and a comparison of the state model approximations generated with each method are discussed by the use of two proposed indices. The comparison is performed with an example case of a realistic aircraft. Model size and fit accuracy of the various methods will be used to compare them with a frequency response direct solution.

II. RFA Techniques

Jones[1] first used rational Laplace transfer functions to approximate the Theodorsen function for the determination for unsteady, incompressible air loading. The most basic form of RFA would be to approximate each element of the GAF matrices by rational Laplace domain transfer functions. As will be discussed, this term-by-term approximation method increases the size of a state-space representation of an nth-order nominal system by mn^2 states, where m is the number of aerodynamic roots required to match each term of the GAF matrices. Roger[2] introduced a method that improves the computational efficiency over the term-by-term method by the use of common denominator roots in the approximation. The matrix Padé approximation technique was introduced by Vepa (see Ref. 3), modified by Edwards (see Ref. 4), and further modified by Karpel, who introduced a minimum-state approximation method (see Refs. 5–8). The minimum-state technique uses nonlinear least-squares optimization to provide the greatest accuracy per lag state introduced into the system.

A. Roger's Approximation

Roger used the following approximation to the aerodynamic force matrix

$$\boldsymbol{Q}(s')\boldsymbol{x}(s) \approx \left(\boldsymbol{P}_0 + \boldsymbol{P}_1 s' + \boldsymbol{P}_2 s'^2 + \sum_{j=3}^{N} \frac{\boldsymbol{P}_j s'}{s' + \gamma_{j-2}}\right)\boldsymbol{x}(s)$$

$$= \left(\boldsymbol{P}_0 + \boldsymbol{P}_1 s' + \boldsymbol{P}_2 s'^2\right)\boldsymbol{x}(s) + \sum_{j=3}^{N} \boldsymbol{P}_j \boldsymbol{x}_{\mathrm{aj}}(s') \tag{3}$$

The term $\boldsymbol{x}_{\mathrm{aj}}(s')$ on the right-hand side of Eq. (3) represents the lag states of the system that are introduced by the approximation. The matrices $\boldsymbol{P}_j$ in Eq. (3) are determined by least-squares optimization to approximate the known aerodynamic forcing data. The form of the lag states $\boldsymbol{x}_{\mathrm{aj}}$ is then

$$\boldsymbol{x}_{\mathrm{aj}}(s) = \{s/[s + (V/b)\gamma_{j-2}]\}\boldsymbol{x}(\boldsymbol{s}) \tag{4}$$

This definition shows that each lag state vector in a system of nominal order n is itself an $(n \times 1)$ vector. Thus, each lag state vector that is added to the system increases the order of the state-space representation of the system by n elements. By the use of Roger's approximation, the GFE in the Laplace domain is,

$$[\boldsymbol{M}s^2 + \boldsymbol{C}s + \boldsymbol{K}]\boldsymbol{x}(\boldsymbol{s}) = \bar{\boldsymbol{q}}[\boldsymbol{Q}(\boldsymbol{s}')]\boldsymbol{x}(\boldsymbol{s})$$

$$= \bar{q}\left[\left(\boldsymbol{P}_0 + \boldsymbol{P}_1 s' + \boldsymbol{P}_2 s'^2\right)\boldsymbol{x}(\boldsymbol{s}) + \sum_{\boldsymbol{j=3}}^{N} \boldsymbol{P}_{\boldsymbol{j}} \boldsymbol{x}_{\mathrm{aj}}(\boldsymbol{s}')\right] \tag{5}$$

The state-space form of the equations of motion for the system, again without consideration of control surface inputs, can then easily be determined:

$$\begin{pmatrix} \dot{\boldsymbol{x}} \\ \ddot{\boldsymbol{x}} \\ \dot{\boldsymbol{x}}_{a3} \\ \vdots \\ \dot{\boldsymbol{x}}_{aN} \end{pmatrix}$$

$$= \begin{bmatrix} 0 & \boldsymbol{I} & 0 & \cdots & 0 \\ -\boldsymbol{M}'^{-1}\boldsymbol{K}' & -\boldsymbol{M}'^{-1}\boldsymbol{C}' & \bar{q}\boldsymbol{M}'^{-1}\boldsymbol{P}_3 & \cdots & \bar{q}\boldsymbol{M}'^{-1}\boldsymbol{P}_N \\ 0 & \boldsymbol{I} & -(V/b)\gamma_1\boldsymbol{I} & & 0 \\ \vdots & \vdots & & \ddots & \\ 0 & \boldsymbol{I} & 0 & & -(V/b)\gamma_{N-2}\boldsymbol{I} \end{bmatrix}$$

$$\times \begin{pmatrix} \boldsymbol{x} \\ \dot{\boldsymbol{x}} \\ \boldsymbol{x}_{a3} \\ \vdots \\ \boldsymbol{x}_{aN} \end{pmatrix}, \qquad \boldsymbol{M}' = \boldsymbol{M} - \bar{q}(b/V)^2\boldsymbol{P}_2$$

$$\boldsymbol{B}' = \boldsymbol{C} - \bar{q}(b/V)\boldsymbol{P}_1, \quad \boldsymbol{K}' = \boldsymbol{K} - \bar{q}\boldsymbol{P}_0 \tag{6}$$

Because the addition of each lag parameter adds n states to an n-order system, the resulting state-space model is of order $2n + (N-2)n = Nn$.

The difference between Roger's approximation method and the term-by-term method is that Roger added the constraint of using common denominator roots for all elements of the GAF matrices. The term-by-term approach allows each element of the GAF matrices to be fit with distinct lag parameters. Because each distinct lag parameter adds an $(n \times 1)$ vector to the resulting state-space model, the approximation of an n-order nominal model with each element of the GAF matrices approximated with m lag parameters would result in a final state-space model of order $2n + mn^2$.

B. Matrix Padé Approximation

The matrix Padé approximation was introduced by Vepa[3] to minimize the number of lag states needed to model the GAF matrices

accurately. Vepa chose the following form for the approximation:

$$\boldsymbol{Q}(s') \approx \left[\boldsymbol{P}_1 s'^2 + \boldsymbol{P}_2 s' + \boldsymbol{P}_3\right][s'\boldsymbol{I} - \boldsymbol{R}]^{-1} \tag{7}$$

Edwards[4] modified the form of the matrix Padé approximation because Vepa's form has proven to be numerically troublesome when attempts were made to cast the aeroelastic model into a state-space form. Edwards used the following reformulation to approximate the aerodynamic forcing matrix:

$$\boldsymbol{Q}(s') \approx [s'\boldsymbol{I} - \boldsymbol{R}]^{-1}\left[\boldsymbol{P}_1 s'^2 + \boldsymbol{P}_2 s' + \boldsymbol{P}_3\right] \tag{8}$$

The unknown coefficient matrix $\boldsymbol{R}$ is determined by the use of least-squares techniques. The matrices $\boldsymbol{P}_j$ can be expressed in terms of the matrix $\boldsymbol{R}$, and the known steady-state and oscillatory values of the aerodynamic force matrix. To satisfy the steady-state condition ($s' = 0$), the matrix $\boldsymbol{P}_3$ is determined as

$$\boldsymbol{Q}(0) = \boldsymbol{Q}^R(0) + j\boldsymbol{Q}^I(0) = \boldsymbol{Q}^R(0) = -\boldsymbol{R}^{-1}\boldsymbol{P}_3 \Rightarrow \boldsymbol{P}_3 = -\boldsymbol{R}\boldsymbol{Q}^R(0)$$

The matrices $\boldsymbol{P}_1$ and $\boldsymbol{P}_2$ are determined by substitution of $s' = jk_i$ into the approximation for $\boldsymbol{Q}(s')$ and separation of real and imaginary parts of the equation:

$$\boldsymbol{P}_1 = \boldsymbol{R}\left[\boldsymbol{Q}^R(k_{f1}) - \boldsymbol{Q}^R(0)\right]\Big/k_{f1}^2 + \boldsymbol{Q}^I(k_{f1})\Big/k_{f1}$$

$$\boldsymbol{P}_2 = \boldsymbol{Q}^R(k_{f2}) - \boldsymbol{R}\left[\boldsymbol{Q}^I(k_{f2})\right]\Big/k_{f2}$$

The values of k_{f1} and k_{f2} are selected from the values of k for which the tabulated aerodynamic force data are available. Which of the k_f are to be chosen is at the discretion of the user. Enforcement of the constraint $k_i = k_{f1} = k_{f2}$ will cause the fit to be exact at k_i, but will result in lower fit accuracy at other values of k. The least-squares determination of $\boldsymbol{R}$ proceeds by the approximations $\boldsymbol{P}_1(k_i) \cong \boldsymbol{P}_1(k_{r1})$ and $\boldsymbol{P}_2(k_i) \cong \boldsymbol{P}_2(k_{r2})$ for all other k_i. In this case, k_{r1} and k_{r2} are chosen from the k for which the tabulated aerodynamic data are available. The choice of which values of k to use for k_{fi} and k_{ri} will affect the least-squares fit accuracy. A general guideline for these choices is to choose them in the range of k where accuracy is most important.

The GFE for a system in which the given matrix Padé approximation is used can be written in the following manner:

$$[\boldsymbol{M}s^2 + \boldsymbol{C}s + \boldsymbol{K}]\boldsymbol{x}(s) = \bar{q}[\boldsymbol{Q}(s')]\boldsymbol{x}(s)$$

$$= \bar{q}[s'\boldsymbol{I} - \boldsymbol{R}]^{-1}\left[\boldsymbol{P}_1 s'^2 + \boldsymbol{P}_2 s' + \boldsymbol{P}_3\right]\boldsymbol{x}(s) \tag{9}$$

The lag states are then

$$\boldsymbol{x}_a = \boldsymbol{Q}(s')\boldsymbol{x}(s) = [s'\boldsymbol{I} - \boldsymbol{R}]^{-1}\left[\boldsymbol{P}_1 s'^2 + \boldsymbol{P}_2 s' + \boldsymbol{P}_3\right]\boldsymbol{x}(s) \tag{10}$$

The state-space model can then be written in the following form

$$\begin{bmatrix} \dot{\boldsymbol{x}} \\ \ddot{\boldsymbol{x}} \\ \dot{\boldsymbol{x}}_a \end{bmatrix} = \begin{bmatrix} \boldsymbol{0} & \boldsymbol{I} & \boldsymbol{0} \\ -\boldsymbol{M}^{-1}\boldsymbol{K} & -\boldsymbol{M}^{-1}\boldsymbol{C} & \bar{q}\boldsymbol{M}^{-1} \\ (V/b)\boldsymbol{P}_3 - \boldsymbol{P}_1'\boldsymbol{K} & \boldsymbol{P}_2 - \boldsymbol{P}_1'\boldsymbol{C} & (V/b)\boldsymbol{R} + \bar{q}\boldsymbol{P}_1' \end{bmatrix} \begin{bmatrix} \boldsymbol{x} \\ \dot{\boldsymbol{x}} \\ \boldsymbol{x}_a \end{bmatrix} \tag{11}$$

where $\boldsymbol{P}_1' = (b/V)\boldsymbol{P}_1\boldsymbol{M}^{-1}$.

For an n-order nominal system, note that the resulting state-space representation is of order $3n$. This provides an improvement in computational efficiency over the term-by-term approximation and Roger's method, whose state-space representations have orders of ($2n + mn^2$) and (Nn), respectively.

Karpel modified the matrix Padé approximation to achieve a model of even lower order, that is, introduction of less aerodynamic lag states to the system, while preserving the accuracy of the approximation.

C. Karpel's Minimum-State Method

The idea behind the minimum-state method is to reduce the number of lag states in the state-space representation given earlier for the matrix Padé method by redefinition of the lag states in such a way so as not to affect the definition of the structural states.

For a system of nominal order n, the matrix Padé method gives a state-space representation of order $3n$ ($2n$ structural states plus the introduction of an ($n \times 1$) vector of lag states to the system). One advantage of the minimum-state method over matrix Padé is that the lag states can be represented by an ($m \times 1$) ($m < n$) lag state vector rather than an ($n \times 1$) lag state vector. The minimum-state method allows the user to choose the number of lag states desired in approximating the GAF matrices.

Begin with the matrix Padé form of the state-space model for the aircraft. Then a transformation is applied to the lag state vector to resolve the aerodynamic state-space coefficients into terms whose structural and aerodynamic contributions are separate. This allows a redefinition of the lag states while ensuring that the structural states go unchanged.

After a transformation and redefinition of the lag states, the matrix Padé state-space realization is recast into the form given by Karpel:

$$\begin{bmatrix} \dot{\boldsymbol{x}} \\ \ddot{\boldsymbol{x}} \\ \dot{\boldsymbol{x}}_a \end{bmatrix} = \begin{bmatrix} \boldsymbol{0} & \boldsymbol{I} & \boldsymbol{0} \\ -(\boldsymbol{M}+\boldsymbol{M}_a)^{-1}(\boldsymbol{K}+\boldsymbol{K}_a) & -(\boldsymbol{M}+\boldsymbol{M}_a)^{-1}(\boldsymbol{C}+\boldsymbol{C}_a) & (\boldsymbol{M}+\boldsymbol{M}_a)^{-1}\boldsymbol{D} \\ 0 & \boldsymbol{E} & \boldsymbol{R} \end{bmatrix} \times \begin{bmatrix} \boldsymbol{x} \\ \dot{\boldsymbol{x}} \\ \boldsymbol{x}_a \end{bmatrix} \tag{12}$$

The aerodynamic time lags for the system are represented by the eigenvalues of the matrix $\boldsymbol{R}$. This representation leads to the following form for the approximation of the aerodynamic force approximation:

$$\boldsymbol{Q}(s') \approx \boldsymbol{P}_1 s'^2 + \boldsymbol{P}_2 s' + \boldsymbol{P}_3 + \boldsymbol{D}'(s'\boldsymbol{I} - \boldsymbol{R}')^{-1}\boldsymbol{E}'s' \tag{13}$$

The parameters in the two preceding equations are related in the following manner:

$$\boldsymbol{M}_a = -1/2\rho b\boldsymbol{P}_1, \qquad \boldsymbol{B}_a = -1/2\rho bV\boldsymbol{P}_2$$

$$\boldsymbol{K}_a = -1/2\rho V^2\boldsymbol{P}_3, \qquad \boldsymbol{D} = 1/2\rho V^2\boldsymbol{D}'$$

$$\boldsymbol{E} = \boldsymbol{E}', \qquad \boldsymbol{R} = (V/b)\boldsymbol{R}'$$

The unknown coefficient matrices $\boldsymbol{D}$ and $\boldsymbol{E}$ are determined through a nonlinear least-squares iteration. The diagonal $\boldsymbol{R}$ matrix is initially user defined and can be updated based on the $\boldsymbol{D}$ and $\boldsymbol{E}$ matrices, once determined. The aerodynamic approximation is constrained to match the known aerodynamic data at $k = 0$ and $k = k_f$. The user chooses k_f from the set of frequencies for which the tabulated aerodynamic data are known. The $\boldsymbol{P}_j$ matrices are expressed in terms of these unknown matrices and known steady-state and oscillatory values of the aerodynamic data in the following manner:

$$\boldsymbol{P}_1 = \left(\boldsymbol{Q}^R(0) - \boldsymbol{Q}^R(k_f)\right)\Big/k_f^2 + \boldsymbol{D}'\left(k_f^2\boldsymbol{I} + \boldsymbol{R}'^2\right)^{-1}\boldsymbol{E}'$$

$$\boldsymbol{P}_2 = \boldsymbol{Q}^I(k_f)\Big/k_f + \boldsymbol{D}'\left(k_f^2\boldsymbol{I} + \boldsymbol{R}'^2\right)^{-1}\boldsymbol{R}'\boldsymbol{E}', \qquad \boldsymbol{P}_3 = \boldsymbol{Q}^R(0)$$

First, a diagonal $\boldsymbol{R}'$ matrix with m distinct diagonal elements is chosen. (These diagonal elements are the user-defined lag parameters for the approximation.) The determination of the unknown matrices $\boldsymbol{D}'$ and $\boldsymbol{E}'$ proceeds by an iterative least-squares procedure, wherein, for all tabulated k_i, except $k = 0$ and the k_f chosen, the approximations $\boldsymbol{P}_1(k_i) \cong \boldsymbol{P}_1(k_f)$ and $\boldsymbol{P}_2(k_i) \cong \boldsymbol{P}_2(k_f)$ form the least-squares problem to be solved. The $\boldsymbol{R}'$ matrix can then be modified to minimize the least-squared error between the approximation and the tabulated aerodynamic data. $\boldsymbol{D}'$ and $\boldsymbol{E}'$ are then modified based on the updated $\boldsymbol{R}'$ matrix, and the procedure is repeated until a user-defined level of convergence is reached.

III. Time Domain State-Space Modeling

Although rational function approximation of the GAF matrices has proven to be a very useful tool in the determination of a state-space representation of the aeroelastic model, the addition of lag states to the system is a hindrance to computational efficiency. The desire for an aeroelastic state-space modeling technique that does not necessitate the addition of lag states to the model has led to the development of FAMUSS and the *P*-transform techniques.

FAMUSS is an equivalent systems approach to state-space modeling. The elements of the state-space matrices are determined by a *p-k* flutter solution and linear and nonlinear least-square fits of the direct solution of the system's transfer function frequency response over the reduced frequency range of interest. The direct solution is determined by interpolation of the GAF matrices between the tabulated values obtained from the oscillatory aerodynamic analysis.

The *P*-transform technique was originally described by Heimbaugh[11] and developed by Winther et al.[12] The *P*-transform technique uses the results of the *p-k* flutter solution[18] to assemble the state-space model for an aeroelastic system.

A. FAMUSS

FAMUSS uses linear and nonlinear curve fitting techniques to match the frequency response of an aircraft for a given flight condition and trajectory. The results of the curve fit are used to generate a state-space model for the aircraft. The advantage of the use of FAMUSS over RFA for the generation of a state-space model of the aircraft is that the FAMUSS model is, for the same level of accuracy, generally of significantly lower order.

FAMUSS generates the state-space model of the aircraft by matching the transfer function frequency response of the system. The GFE are manipulated to give the transfer function frequency response

$$\boldsymbol{H}_x(s) = \boldsymbol{x}(s)/\boldsymbol{u}(s)$$

$$= [\boldsymbol{M}s^2 + \boldsymbol{C}s + \boldsymbol{K} - \bar{q}\boldsymbol{Q}(s')]^{-1}\left[-\boldsymbol{M}s^2 + \bar{q}\boldsymbol{Q}_\delta(s')\right] \tag{14}$$

The modal response of the preceding equation is multiplied by the system mode shapes ($\boldsymbol{\Phi}_{\text{Sen}}$) to obtain the response in physical coordinates:

$$\boldsymbol{H}(s) = \frac{\boldsymbol{y}(s)}{\boldsymbol{u}(s)} = \frac{\boldsymbol{\Phi}_{\text{Sen}}\boldsymbol{x}(s)}{\boldsymbol{u}(s)} = \boldsymbol{\Phi}_{\text{Sen}}\boldsymbol{H}_x(s) \tag{15}$$

The transfer function frequency response of the system is determined by the solution of Eq. (15) over a range of reduced frequency. The GAF matrices are determined at each value of reduced frequency of interest by interpolation over the tabulated set of reduced frequency data.

FAMUSS uses the block diagonal, phase variable form for the state matrices:

$$\dot{\boldsymbol{x}}(t) = \begin{bmatrix} 0 & 1 & \\ a_{21} & a_{22} & \\ & & \ddots \end{bmatrix}\boldsymbol{x}(t) + \begin{bmatrix} 0 & b_{12} & \cdots \\ 1 & b_{22} & \cdots \\ \vdots & \vdots & \end{bmatrix}\boldsymbol{u}(t)$$

$$\boldsymbol{y}(t) = \begin{bmatrix} c_{11} & c_{12} & \cdots \\ c_{21} & c_{22} & \cdots \\ \vdots & \vdots & \end{bmatrix}\boldsymbol{x}(t) + \begin{bmatrix} d_{11} & d_{12} & \cdots \\ d_{21} & d_{22} & \cdots \\ \vdots & \vdots & \end{bmatrix}\boldsymbol{u}(t)$$

The approximation to the transfer function frequency response for the state-space model is

$$\hat{\boldsymbol{H}}(s) = \boldsymbol{C}[s\boldsymbol{I} - \boldsymbol{A}]^{-1}\boldsymbol{B} + \boldsymbol{D} \tag{16}$$

In this form, each block can be approximated separately, and the blocks can be summed to form the total state-space model. The form of the approximation for the i, jth element of the known transfer matrix (truth model) is

$$\hat{h}_{ij}(s) = \sum_{m=1}^{n_b} \frac{\hat{h}^m_{Nij}(s)}{\hat{h}^m_{Dij}(s)} + d_{ij}$$

where n_b is the mode or block number; $i, j = (1, 2)$ correspond to the position in the 2×2 block m and

$$\hat{h}^m_{Nij}(s) = \left(c^m_{i1}b^m_{ij} + c^m_{i2}b^m_{2j}\right)s + \left(c^m_{i2}b^m_{1j} - c^m_{i1}b^m_{ij}a^m_{22} + c^m_{i1}b^m_{2j}a^m_{21}\right)$$

$$\hat{h}^m_{Dij}(s) = s^2 - a^m_{22}s - a^m_{21}$$

The formation of the state-space model in FAMUSS is a three-step iterative procedure.

1. *Step 1: Formulation of the State Matrix, p-k Flutter Solution*

First the state matrix $\boldsymbol{A}$ is determined by performance of a *p-k* flutter solution on the free response equations of motion, that is, the control surface forcing is neglected. Because the state-space model is in the block diagonal phase variable form, the blocks of the $\boldsymbol{A}$ matrix are composed of the real and imaginary parts of the system roots in the following manner

$$a^m_{21} = -(\omega^m)^2, \qquad a^m_{22} = -2(\zeta^m)(\omega^m)$$

where ω^m is the flutter frequency of mode m, and ζ^m is the modal damping ratio of mode m.

2. *Step 2: Formulation of State Matrices* B, C, *and* D

Once the $\boldsymbol{A}$ matrix is determined from a *p-k* flutter solution or equivalent method, an iterative technique is performed to determine the $\boldsymbol{B}$, $\boldsymbol{C}$, and $\boldsymbol{D}$ matrices to match the given response. There are two steps to this process. The first step is the predictor step. The second step is the corrector step.

a. Step 2.1: model prediction. There are two parts to the predictor step. First, initial values of the $\boldsymbol{C}$ matrix and the first column of the $\boldsymbol{D}$ matrix are determined by consideration of the system response due only to the first system input. This leads to the following equation, for $i = 1$ to n_b:

$$\hat{h}_{i1}(s) = [c_{i1} \quad c_{i2} \quad \cdots][s\boldsymbol{I} - \boldsymbol{A}]^{-1}\begin{bmatrix} 0 \\ 1 \\ \vdots \end{bmatrix} + d_{i1} \tag{17}$$

The column vector of alternating ones and zeros in Eq. (17) is the first column of the $\boldsymbol{B}$ matrix for the system. It has this form because of the phase variable form chosen for the $\boldsymbol{A}$ matrix. A linear least-squares fit is applied to this equation to match the approximate system response with the calculated response. Because these fits are based on the first system input only, the elements of the $\boldsymbol{C}$ and $\boldsymbol{D}$ matrices will cause the system transfer matrix to match the transfer functions corresponding to the first input more accurately than the transfer functions corresponding to the other system inputs.

By the use of the $\boldsymbol{C}$ matrix determined from the preceding fit, the remaining columns of the $\boldsymbol{B}$ and $\boldsymbol{D}$ matrices are determined based on the rest of the system inputs with the following equation, for a particular j, one column at a time:

$$\begin{bmatrix} \hat{h}_{1j}(s) \\ \hat{h}_{2j}(s) \\ \vdots \end{bmatrix} = \boldsymbol{C}[s\boldsymbol{I} - \boldsymbol{A}]^{-1}\begin{bmatrix} b_{1j} \\ b_{2j} \\ \vdots \end{bmatrix} + \begin{bmatrix} d_{1j} \\ d_{2j} \\ \vdots \end{bmatrix} \tag{18}$$

Again, a linear least-squares fit is applied to determine all columns of the $\boldsymbol{B}$ and $\boldsymbol{D}$ matrices that best match the transfer function frequency responses. The $\boldsymbol{B}$, $\boldsymbol{C}$, and $\boldsymbol{D}$ matrices are now full. The $\boldsymbol{C}$ matrix elements are based only on the output due to the first system input though. To obtain a state-space model with matrices whose elements

are to be accurate over all system inputs, the model is corrected as follows.

b. Step 2.2: model correction. The $\boldsymbol{C}$ and $\boldsymbol{D}$ matrix estimates can be improved over all system inputs by performing another linear least-squares fit. The $\boldsymbol{B}$ matrix that was determined from fitting the preceding equation to the truth model transfer function frequency response is used to update the $\boldsymbol{C}$ and $\boldsymbol{D}$ matrices by the use of Eq. (19):

$$\lfloor \hat{h}_{i1}(s) \quad \hat{h}_{i2}(s) \quad \cdots \rfloor = [c_{i1} \quad c_{i2} \quad \cdots][s\boldsymbol{I} - \boldsymbol{A}]^{-1}\boldsymbol{B} + [d_{i1} \quad d_{i2} \quad \cdots] \tag{19}$$

The $\boldsymbol{C}$ matrix elements are now less accurate for the first system input but more accurate across all system inputs. Equations (18) and (19) are repeated iteratively until a converged solution for the $\boldsymbol{B}$, $\boldsymbol{C}$, and $\boldsymbol{D}$ matrices is achieved. The fit of the transfer function frequency response is further improved by the addition of block diagonal values to the A matrix and when those values are refined through the use of a nonlinear least-squares curve fitting technique, as shown next. These added terms are equivalent to lag states.

c. Step 3: nonlinear model optimization. The $\boldsymbol{A}$ matrix is based on the poles of the free response of the system, the p-k flutter solution. As in other methods, the addition of lag states can improve the approximation. These are easily added as additional blocks in the $\boldsymbol{A}$ matrix. A nonlinear optimization algorithm in FAMUSS is used to improve the terms in the added blocks of the $\boldsymbol{A}$ matrix. The technique used to perform this optimization is a modified Leavenberg–Marquardt algorithm.

FAMUSS provides accurate, low-order approximations of the state-space representation of aeroelastic models. FAMUSS also has the capacity to introduce lag states to the system to improve fit accuracy. One limitation to the FAMUSS technique is that it is limited in the number of input–output combinations for which it can provide a reliable, linear, time-invariant state-space model approximation. The main limitation of FAMUSS is that the process does not preserve the definition of the original system states. The preservation of the system states is necessary to perform a residualization process wherein the linear, quasi-steady portion of the $\boldsymbol{A}$ and $\boldsymbol{B}$ state-space matrices is replaced with a set of nonlinear, quasi-steady equations that are based on experimental results. The nonlinear portion that is added to the model is based on flight-test data or wind-tunnel data. It is, therefore, more accurate than the model predicted by the linear aerodynamic analysis. The P-transform method accommodates this residualization because it provides a state-space representation for the aeroelastic system while maintaining the definitions of the structural states.

B. *P*-Transform Technique

Under the assumption of a harmonic solution, the GAF matrices can be decomposed as

$$\begin{aligned}\boldsymbol{Q}(s')\boldsymbol{x}(s) &= [\boldsymbol{Q}^R(s') + j\boldsymbol{Q}^I(s')]\boldsymbol{x}(s) \\ &= \boldsymbol{Q}^R(s')\boldsymbol{x}(s) + [(\bar{c}/2V)\boldsymbol{Q}^I(s')/k]\dot{\boldsymbol{x}}(s)\end{aligned} \tag{20}$$

For a fixed flight condition, the GFE [Eq. (1)] can then be written in state-space form as

$$\begin{aligned}\begin{pmatrix}\ddot{\boldsymbol{x}} \\ \dot{\boldsymbol{x}}\end{pmatrix} &= \begin{pmatrix}\boldsymbol{M}^{-1}(\bar{q}(\bar{c}/2V)\boldsymbol{Q}^I(k)/k - \boldsymbol{C}) & \boldsymbol{M}^{-1}(\bar{q}\boldsymbol{Q}^R(k) - \boldsymbol{K}) \\ \boldsymbol{I} & 0\end{pmatrix}\begin{pmatrix}\dot{\boldsymbol{x}} \\ \boldsymbol{x}\end{pmatrix} \\ &+ \begin{pmatrix}-\boldsymbol{M}^{-1}\boldsymbol{M}_\delta & \boldsymbol{M}^{-1}(\bar{q}(\bar{c}/2V)\boldsymbol{Q}^I_\delta(k)/k) & \boldsymbol{M}^{-1}\left(\bar{q}\boldsymbol{Q}^R_\delta(k)\right) \\ 0 & 0 & 0\end{pmatrix} \\ &\times \begin{pmatrix}\ddot{\boldsymbol{\delta}} \\ \dot{\boldsymbol{\delta}} \\ \boldsymbol{\delta}\end{pmatrix}\end{aligned} \tag{21}$$

For simplicity, the preceding equations will be expressed as follows:

$$\dot{\boldsymbol{X}} = \boldsymbol{A}(k)\boldsymbol{X} + \boldsymbol{B}(k)\boldsymbol{U} \tag{22}$$

where $\boldsymbol{X} = (\dot{\boldsymbol{x}} \;\; \boldsymbol{x})^T$ and $\boldsymbol{U} = (\ddot{\boldsymbol{\delta}} \;\; \dot{\boldsymbol{\delta}} \;\; \boldsymbol{\delta})^T$.

This representation is not LTI because the GAF matrices are a function of the reduced frequency $k = \omega b/V$. The P-transform technique is used to eliminate the frequency dependence of the state matrices, resulting in an LTI approximation of the state-space representation for the GFE.

The process begins with a p-k flutter solution of the GFE. The GAF matrices are then determined at each of the p-k flutter roots, which leads to the state-space model for the system at each of the flutter frequencies. This results in a set of state-space representations for the system that are each accurate in the vicinity of the reduced frequency for which they are constructed:

$$\dot{\boldsymbol{X}} = \boldsymbol{A}(k_i)\boldsymbol{X} + \boldsymbol{B}(k_i)\boldsymbol{U} \tag{23}$$

where $i = 1$, the number of system modes. For each k_i, the system representation can be decoupled through a similarity transform of the states. The modal response of the pertinent mode can then be determined.

Let $\boldsymbol{T}(k_i)$ be the matrix of eigenvectors of $\boldsymbol{A}(k_i)$. The transformation $\boldsymbol{X} = \boldsymbol{T}(k_i)\boldsymbol{P}$ gives, after premultiplication by $\boldsymbol{T}^{-1}(k_i)$,

$$\dot{\boldsymbol{P}} = \bar{\boldsymbol{A}}(k_i)\boldsymbol{P} + \bar{\boldsymbol{B}}(k_i)\boldsymbol{U}$$

where $\bar{\boldsymbol{A}}(k_i) = \boldsymbol{T}(k_i)^{-1}\boldsymbol{A}(k_i)\boldsymbol{T}(k_i)$ is a diagonal matrix of complex conjugate eigenvalues, and $\bar{\boldsymbol{B}}(k_i) = \boldsymbol{T}(k_i)^{-1}\boldsymbol{B}(k_i)$, where $\boldsymbol{T}(k_i)$ is a full matrix of complex conjugate eigenvectors.

Because the elements of the final system model should be noncomplex, both the matrices $\bar{\boldsymbol{A}}(k_i)$ and $\boldsymbol{T}(k_i)$ are converted from complex diagonal to real block diagonal for all k_i. This gives $\bar{\boldsymbol{A}}_R(k_i)$ as real block diagonal with 2×2 submatrices down the diagonal, with the real parts of the eigenvalues on the diagonals and the imaginary parts on the off-diagonals. The $\boldsymbol{T}_R(k_i)$ matrices are real with each pair of complex conjugate eigenvalue columns replaced with a pair of real coefficient vectors.[11]

All of the converged eigenvalue blocks of $\bar{\boldsymbol{A}}_R(k_i)$ are gathered into the block diagonal of a new matrix $\hat{\boldsymbol{A}}(k_i)$. The corresponding eigenvector column pairs in $\boldsymbol{T}_R(k_i)$ are gathered into the new matrix $\hat{\boldsymbol{T}}(k_i)$. The corresponding row pairs of $\bar{\boldsymbol{B}}(k_i) = \boldsymbol{T}_R(k_i)^{-1}\boldsymbol{B}(k_i)$ are gathered into the $\hat{\boldsymbol{B}}$ matrix.

We now have the following equation expressed in p-domain coordinates:

$$\dot{\boldsymbol{P}} = \hat{\boldsymbol{A}}\boldsymbol{P} + \hat{\boldsymbol{B}}\boldsymbol{U} \tag{24}$$

This equation is transformed back to the modal coordinates,

$$\boldsymbol{x} = \hat{\boldsymbol{T}}\boldsymbol{P} \Rightarrow \boldsymbol{P} = \hat{\boldsymbol{T}}^{-1}\boldsymbol{X}$$

Through this substitution and by premultiplication by $\hat{\boldsymbol{T}}$,

$$\dot{\boldsymbol{X}} = \tilde{\boldsymbol{A}}\boldsymbol{X} + \tilde{\boldsymbol{B}}\boldsymbol{U}$$

where $\tilde{\boldsymbol{A}} = \hat{\boldsymbol{T}}\hat{\boldsymbol{A}}\hat{\boldsymbol{T}}^{-1}$ and $\tilde{\boldsymbol{B}} = \hat{\boldsymbol{T}}\hat{\boldsymbol{B}}$. After rearranging the state vector to bring the rigid-body states to the top, this leads to the following LTI form for the equations of motion:

$$\begin{pmatrix}\dot{\boldsymbol{r}} \\ \dot{\boldsymbol{\eta}} \\ \dot{\boldsymbol{\zeta}}\end{pmatrix} = \begin{pmatrix}\boldsymbol{A}_{11} & \boldsymbol{A}_{12} & \boldsymbol{A}_{13} \\ \boldsymbol{A}_{21} & \boldsymbol{A}_{22} & \boldsymbol{A}_{23} \\ 0 & \boldsymbol{I} & 0\end{pmatrix}\begin{pmatrix}\boldsymbol{r} \\ \boldsymbol{\eta} \\ \boldsymbol{\zeta}\end{pmatrix} + \begin{pmatrix}\boldsymbol{B}_1 \\ \boldsymbol{B}_2 \\ 0\end{pmatrix}\begin{pmatrix}\ddot{\boldsymbol{\delta}} \\ \dot{\boldsymbol{\delta}} \\ \boldsymbol{\delta}\end{pmatrix} \tag{25}$$

Here, $\boldsymbol{r}$ is the vector of rigid-body rates and displacements, $\boldsymbol{\eta}$ is the vector of flexible mode rates, and $\boldsymbol{\zeta}$ is the vector of flexible mode displacements.

C. Residualization of the Equations of Motion

Because the definition of the system states is retained, *P*-transform allows the quasi-steady portion of the model pertaining to the rigid-body modes of the system to be separated and replaced with an experimentally determined, nonlinear set of equations. A static residualization method such as Guyan reduction is applied to the system to separate the quasi-steady and dynamic parts of the solution (see Ref. 12):

$$\begin{pmatrix} \dot{\boldsymbol{r}} \\ \dot{\boldsymbol{\eta}} \\ \dot{\boldsymbol{\zeta}} \end{pmatrix} = \underbrace{\begin{pmatrix} \bar{\bar{\boldsymbol{A}}}_{11} \\ 0 \\ 0 \end{pmatrix} \boldsymbol{r} + \begin{pmatrix} \bar{\bar{\boldsymbol{B}}}_{1} \\ 0 \\ 0 \end{pmatrix} \begin{pmatrix} \ddot{\boldsymbol{\delta}} \\ \dot{\boldsymbol{\delta}} \\ \boldsymbol{\delta} \end{pmatrix}}_{\text{Linear}\qquad\text{QSAE}} + \underbrace{\begin{pmatrix} \boldsymbol{A}_{11} & \boldsymbol{A}_{12} & \boldsymbol{A}_{13} \\ \boldsymbol{A}_{21} & \boldsymbol{A}_{22} & \boldsymbol{A}_{23} \\ 0 & \boldsymbol{I} & 0 \end{pmatrix} \begin{pmatrix} \boldsymbol{r} \\ \boldsymbol{\eta} \\ \boldsymbol{\zeta} \end{pmatrix} + \begin{pmatrix} \boldsymbol{B}_{1} \\ \boldsymbol{B}_{2} \\ 0 \end{pmatrix} \begin{pmatrix} \ddot{\boldsymbol{\delta}} \\ \dot{\boldsymbol{\delta}} \\ \boldsymbol{\delta} \end{pmatrix}}_{\text{Linear}\qquad\text{Dynamic}\qquad\text{Aeroelastic}} \tag{26}$$

The linear quasi-steady aeroelastic (QSAE) part of Eq. (26) can now be replaced with the nonlinear model.

IV. Metrics for the Quantification of Approximation Error

To illustrate the application of the techniques reviewed and to compare them, an example case of a realistic aircraft in level flight at an altitude of sea level and a Mach number of 0.2 is considered. The system is considered to have 10 vibration modes, that is, $n = 10$, three symmetric rigid-body modes, and seven asymmetric flexible modes. Tabulated generalized aerodynamic forcing data are available at 20 reduced frequency values. There were 5 control surface inputs and 18 outputs (position, rate, and acceleration of each of the six rigid-body degrees of freedom) modeled. Roll rate per deflection of the control surface 1 (CS1) and vertical load factor N_z per CS1 were chosen as representative input–output combinations for the system. Transfer function frequency responses of these input–output combinations for each of the methods discussed before are shown in Figs. 1–5.

For comparison between the accuracy of the RFA techniques for approximation of the GAF data, a sum of squared errors measure is proposed. This proposed measure J_1 is the square root of the normalized sum of the squared complex distance, denoted by $\varepsilon_{1,ijk}$, between the tabulated GAF data and the predicted values from the RFA [Eq. (27)]. The summation is performed over all of the $n = 10$ system modes and the $k_{\max} = 20$ reduced frequency values for which

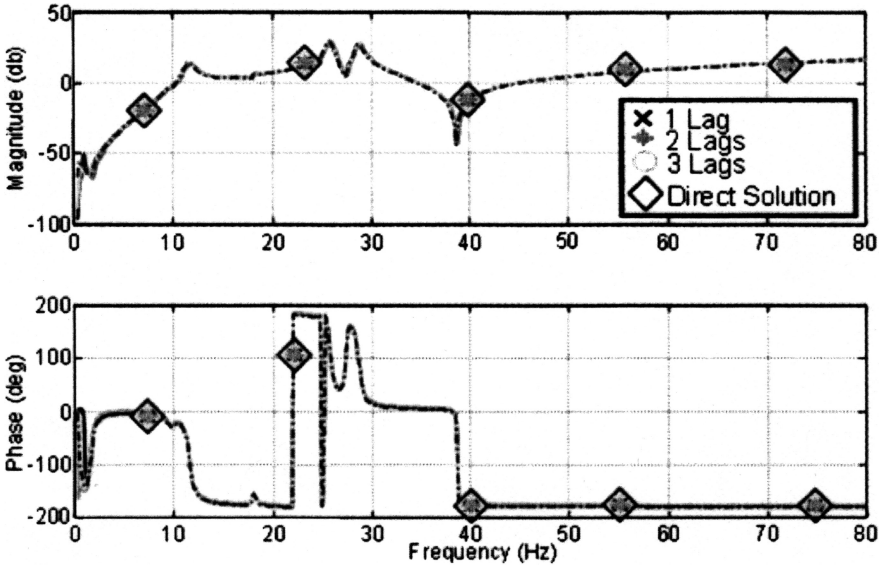

Fig. 1 Roger's method: *Nz* per CS1.

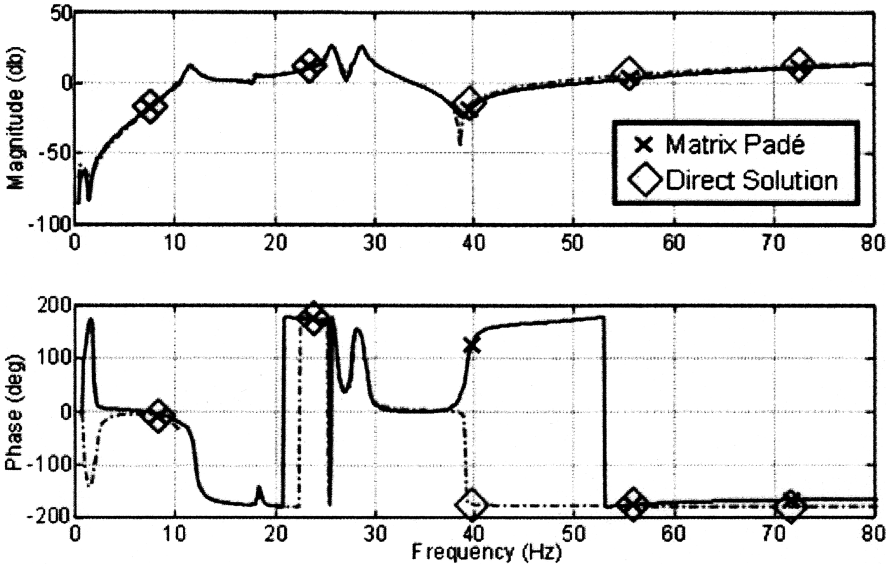

Fig. 2 Matrix Padé method: *Nz* per CS1.

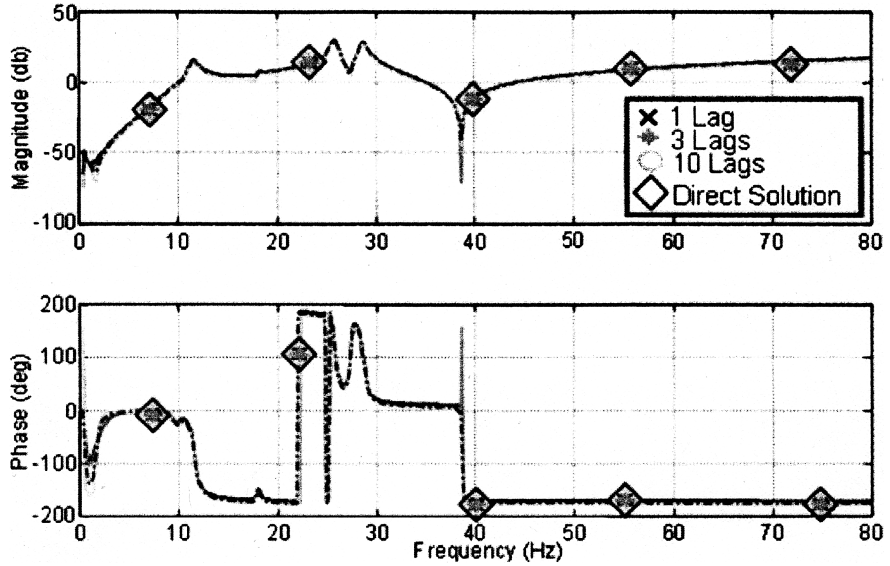

Fig. 3 Minimum-state method: *Nz* per CS1.

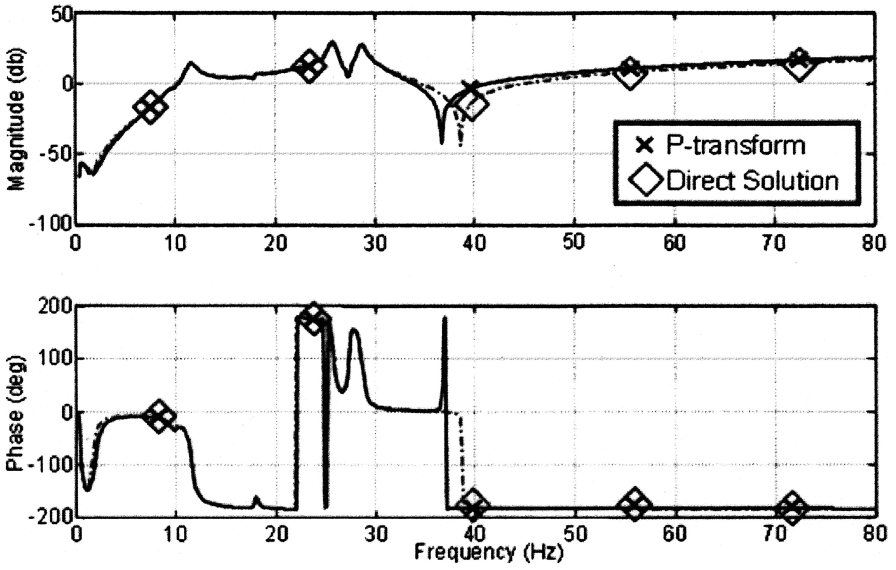

Fig. 4 *P*-transform method: *Nz* per CS1.

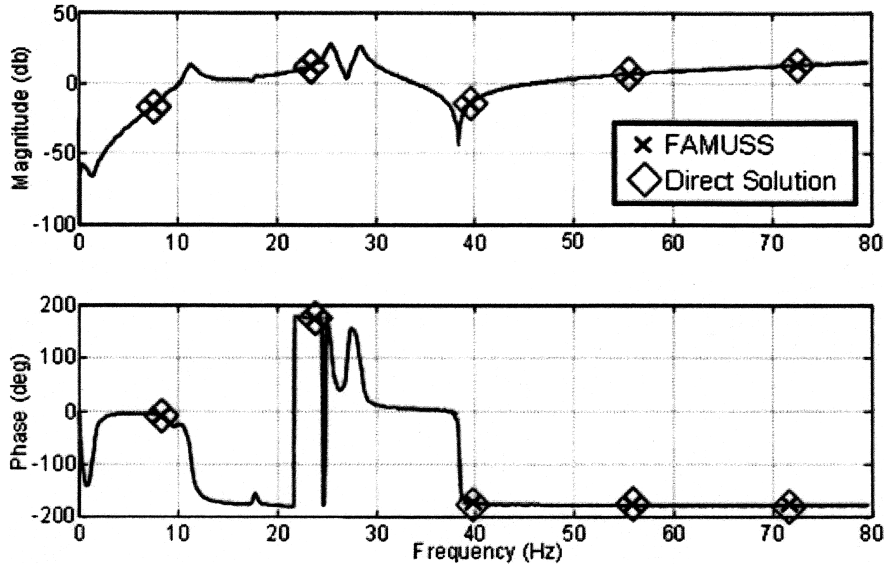

Fig. 5 FAMUSS method: *Nz* per CS1.

the GAF data are tabulated and normalized by $n \times n \times k_{\max} = 2000$ (the number of data points in the $10 \times 10 \times 20$ error matrix):

$$J_1 = \sqrt{\frac{1}{(n \times n \times k_{\max})} \sum_{k=1}^{k_{\max}} \sum_{j=1}^{n} \sum_{i=1}^{n} \varepsilon_{1,ijk}^2} \tag{27}$$

The accuracy of the transfer function frequency response approximations was quantified by another proposed sum of squared errors measure [Eq. (28)]. This measure, J_2, is the square root of the normalized sum of the squared complex distance, denoted by $\varepsilon_{2,ijk}$, between the transfer function frequency responses of the direct solution and those responses predicted by each of the methods considered. J_2 is evaluated at the 20 values of reduced frequency for which tabulated GAF data are available. The summation is performed over the $n_O = 18$ outputs, $n_I = 5$ inputs, and the $k_{\max} = 20$ reduced frequency values and is normalized by $n_O \times n_I \times k_{\max} = 1800$ (the number of data points in the $18 \times 5 \times 20$ error matrix):

$$J_2 = \sqrt{\frac{1}{(n_O \times n_I \times k_{\max})} \sum_{k=1}^{k_{\max}} \sum_{j=1}^{n_I} \sum_{i=1}^{n_O} \varepsilon_{2,ijk}^2} \tag{28}$$

The transfer function response errors for the chosen representative input–output combinations are calculated as before, but normalized by a factor of 40 because they are calculated for two of the transfer functions only.

A. RFA Methods

Roger's RFA approximation was performed over the aerodynamic data with the addition of one, two, and three aerodynamic roots, resulting in state models of order 30, 40, and 50, respectively. Table 1 shows the sum of squared errors and aerodynamic root locations chosen for each of these cases. As the number of lag states used in the RFA is increased, the sum of squared errors is seen to decrease greatly, but at the cost of increased order, as cited.

Table 2 shows the approximation parameters, sum of squared errors and aerodynamic root locations obtained for a matrix Padé RFA of the data, which resulted in a state model of order 30. The sum of squared errors for the matrix Padé RFA result is comparable to that obtained from the Roger's approximation with the introduction of one lag state. For the given example, however, the matrix Padé RFA method produced a lag state matrix that has unstable roots. This may be undesirable in some cases.

Table 1 GAF approximation errors and aerodynamic root locations using Roger's RFA method

	Roger's method	
Aerodynamic root(s)	Sum of squared errors	Root location(s)
One	$3.841655E{+}05$	-271.72
Two	$1.065735E{+}05$	-224.98
		-271.72
Three	$7.774551E{+}04$	-126.53
		-186.03
		-224.98

Table 2 GAF approximation errors and aerodynamic root locations using the matrix Padé RFA method

Sum of squared errors	RFA parameters	Root locations
$3.83325E{+}05$	$kr1 = 0.07$	5446.49
	$kr2 = 36.58$	$919.79 + 1064.61i$
	$kf1 = 224.98$	$919.79 - 1064.61i$
	$kf2 = 224.98$	-540.84
		$272.23 + 139.37i$
		$272.23 - 139.37i$
		$-102.32 + 298.63i$
		$-102.32 - 298.63i$
		-13.55
		-21.66

Table 3 shows the approximation parameters, sum of squared errors, and aerodynamic root locations obtained for the minimum-state approximation method. Systems with 1, 3, and 10 lag states were simulated, resulting in state models of order 21, 24, and 30, respectively. Again, the sum of squared errors of the approximation is seen to decrease as the number of lag states added to the system increased. Compared with Roger's method, the minimum-state method produces a final state model that is much more computationally efficient. This is because the introduction of one lag state by the use of the minimum-state method adds only one state to the final state-space model, whereas the introduction of one lag state when Roger's method is used increases the final state model by 10 states.

Roger's RFA method with one lag state, the matrix Padé method and the minimum-state method with 10 lag states each introduce 10 additional states to the final state-space model. Comparing the sum of squared errors for these cases, it is seen that, for the given example case, the minimum-state method produces the most accuracy per lag state introduced to the system.

B. Transfer Function Responses

The transfer function frequency response matrices were determined for each of the state model generation methods described earlier. These matrices were compared with a direct solution of the data obtained by finding the transfer function frequency responses directly from the GFE data. A cubic spline interpolation was used to approximate the values of the aerodynamic forcing matrices in the frequency range [0, 80] Hz. The frequency response matrix is of dimension 18×5 because there are 18 system outputs for each of the five control surface inputs considered. Table 4 lists the number of aerodynamic roots, the transfer matrix sum of squared errors and

Table 3 GAF approximation errors and aerodynamic root locations using the minimum-state RFA method

	Minimum state method		
Aerodynamic root(s)	kf	Sum of squared errors	Root location
1	$2.71720E{+}02$	$5.33167E{+}05$	-271.72
3	$2.71720E{+}02$	$8.67585E{+}04$	-126.53
			-224.98
			-271.72
10	$2.71720E{+}02$	$7.51394E{+}04$	-1.82
			-6.46
			-13.13
			-22.74
			-36.58
			-56.51
			-85.21
			-126.53
			-186.03
			-271.72

Table 4 State model transfer function FRA errors

Number of aerodynamic roots	Total transfer matrix sum of squared error	Transfer function sum of squared error
	Roger's method	
1	$1.88613E{-}01$	$1.01714E{-}02$
2	$2.04537E{-}01$	$1.19551E{-}02$
3	$1.95341E{-}01$	$1.17865E{-}02$
	Matrix Pade' method	
10	$1.46617E{+}00$	$1.36578E{-}01$
	Minimum state method	
1	$3.12659E{-}01$	$1.88850E{-}02$
3	$3.28166E{-}01$	$2.12208E{-}02$
10	$3.36924E{-}01$	$2.20962E{-}02$
	P-transform	
0	$6.18570E{-}01$	$1.13125E{-}01$
	FAMUSS	
0	$3.07017E{-}01$	$6.85141E{-}03$

the sum of the squared errors for the transfer functions shown in Figs. 1–5. The trend of the decreasing approximation error with an increasing number of lag states in the RFA approximations is not seen in the transfer function matrices. This is because the interaction of the approximated aerodynamic forcing matrices with the structural matrices of the GFE could amplify or attenuate the GAF approximation error when the system frequency response is determined. For the given example, Roger's RFA method produced the most accurate match of the state model with the direct solution. The methods considered, listed in order of approximation accuracy for the particular example case are Roger's, FAMUSS, minimum-state, P-transform, and matrix Padé.

V. Conclusions

The test case presented here is not intended to provide a general ranking of the ability of these methods. For that, several different flight conditions and aircraft models would be needed. Instead, the intent is to illustrate, by the use of a real-world example, the results of their implementation along with suggested metrics one could use to quantify their accuracy for a given test case.

A technical review of the methods for the generation of a state-space model has been provided for a flexible aircraft with frequency-varying aerodynamic forcing. Of these, Roger's method, matrix Padé, and Karpel's minimum-state method are all rational function approximation techniques used to generate matrix approximations of the generalized aerodynamic forcing. The resulting matrix approximations can be used in the formation of a state model for the system as described earlier. The P-transform and FAMUSS methods generate state model approximations of the system directly. Two error indices are proposed to compare approximation errors between the various methods.

The RFA methods described entail the introduction of aerodynamic, or lag states, to the system for accurate approximation of the generalized aerodynamic forcing. Neither FAMUSS nor P-transform requires the introduction of additional states. The FAMUSS method includes the option of introducing lag states to the system, whereas the P-transform method does not. No lag states were introduced to the FAMUSS approximation for the example.

A comparison of the RFA techniques (Table 1) shows that the minimum-state method provides the most accuracy in the approximation of the GAFs per lag state used. Table 2 shows that the Roger's RFA method provides the best approximation to the system transfer matrix for the example case. Roger's method also incurs the most penalty in computational efficiency in terms of the increase of model size increase per lag state added, however.

Of the two methods that do not require the introduction of lag states, (FAMUSS and P-transform) FAMUSS has shown to match the direct solution of the GFE more accurately. The drawback to the FAMUSS method is that the process of transfer function fitting does not preserve the aircraft state definitions. This prohibits the use of the residualization process described earlier to replace the linear quasi-steady rigid-body components of the state model with the more accurate, nonlinear components derived from experiment.

An insight from the case studies reported is that an increase in the approximation accuracy of the GAF matrices does not necessarily translate to a more accurate fit of the modeled transfer function response with the direct solution. The proposed error indices could also be used for other possible comparisons. The study highlights the need for improved methods to capture flexibility effects in state modeling techniques. There is a need for improved approaches to correlate errors due to flexibility effects to aircraft physical characteristics, including GAF. Such methods would help develop a better understanding and facilitate development of reliable models for improving prediction accuracies for trajectories and loads in the presence of significant flexibility effects.

Acknowledgments

This research was supported in part by a National Science Foundation GOALI grant (#9979234) which helped the students work at Boeing, St. Louis, Missouri during the term of the research. The authors also gratefully acknowledge the assistance provided by Eric Reichenbach and Charles Goodman of Boeing, St. Louis, Missouri.

References

[1]Jones, R. T., "The Unsteady Lift of a Wing of Finite Aspect Ratio," NACA Rept. 681, 1941.

[2]Roger, K. L., "Airplane Math Modeling Methods for Active Control Design," CP-228, AGARD, Aug. 1977.

[3]Vepa, R., "Finite State Modeling Methods of Aeroelastic Systems," NASA CR-2779, 1977.

[4]Edwards, J. W., "Applications of Laplace Transform Methods to Airfoil Motion and Stability Calculations," AIAA Paper 79-0772, April 1979.

[5]Karpel, M., "Design for Active Flutter Suppression and Gust Alleviation Using State-Space Modeling," *Journal of Aircraft*, Vol. 19, No. 3, 1982, pp. 221–227.

[6]Karpel, M., "Design for Active and Passive Flutter Suppression and Gust Alleviation," Ph.D. Dissertation, Dept. of Aeronautics and Astronautics, Stanford Univ., Stanford, CA, 1980.

[7]Karpel, M., "Size-Reduction Techniques for the Determination of Efficient Aeroservoelastic Models," *Control and Dynamic Systems*, Vol. 54, Academic Press, San Diego, CA, 1992, pp. 263–295.

[8]Karpel, M., and Strul, E., "Minimum-State Unsteady Aerodynamic Approximations with Flexible Constraints," *Journal of Aircraft*, Vol. 33, No. 6, 1996, pp. 1190–1196.

[9]Pitt, D. M., and Goodman, C. E., "FAMUSS: A New Aeroservoelastic Modeling Tool," AIAA Paper 92-2395-CP, 1992.

[10]Goodman, C. E., "Flexible Aircraft Modeling Using State Space (FAMUSS)," McDonnell Douglas, Rept. MDC 94P0047, St. Louis, MO, Dec. 1994.

[11]Heimbaugh, R. M., "Flight Controls Structural Dynamics IRAD," McDonnell Douglas, Rept. MDC J2303, St. Louis, MO, March 1983.

[12]Winther, B. A., Goggin, P. J., and Dykman, J. R., "Reduced Order Dynamic Aeroelastic Model Development and Integration with Nonlinear Simulation," *Journal of Aircraft*, Vol. 37, No. 5, 2000, pp. 833–839.

[13]Marzocca, P., Librescu, L., and Silva, W. A., "Volterra Series Approach for Nonlinear Aeroelastic Response of 2-D Lifting Surfaces," AIAA Paper 2001-1459, April 2001.

[14]Hall, K. C., Thomas, J. P., and Dowell, E. H., "Proper Orthogonal Decomposition Technique for Transonic Unsteady Aerodynamic Flows," *AIAA Journal*, Vol. 38, No. 10, 2000, pp. 1853–1862.

[15]Leishman, J. G., "Principles of Helicopter Aerodynamics," Cambridge Univ. Press, Cambridge, England, U.K., 2000, Chap. 8, pp. 306–371.

[16]Leishman, J., and Crouse, G., "A State-Space Model of Unsteady Aerodynamics in a Compressible Flow for Flutter Analyses," AIAA Paper 89-0022, Jan. 1989.

[17]Nørgaard, M., Jorgensen, C. C., and Ross, J. C., "Neural Network Prediction of New Aircraft Design Coefficients," NASA TM 112197, May 1997.

[18]Hassig, H. J., "An Approximate True Damping Solution of the Flutter Equation by Determinant Iteration," *Journal of Aircraft*, Vol. 8, No. 11, 1971, pp. 885–889.